Modelling of oxydibenzenesulfonyl hydrazide (OBSH) in gas-phase

Bahar Eren[a] and Yelda Yalcin Gurkan[b]*

[a]Faculty of Agriculture, [b]Department of Chemistry,

Tekirdag Namik Kemal University, Tekirdag, Turkey

E-mail: yyalcin@nku.edu.tr

Oxydibenzenesulfonyl hydrazide (OBSH), under some circumstances, can act as a foaming factor, and also as a crosslinking agent in the hardening reaction. Another use of OBSH is elastomer production under room pressure, such as natural rubber, styrene-butadiene rubber, or neoprene; and also in the solidifying reaction of thermoplastic production such as, acrylonitrile butadiene styrene plastics, polyethylene, polystyrene, or polyvinylchloride, and can also be used together with the combinations of resin and rubber. It has considerable advantages in wire and cable production due to its isolatable characteristics. The structural and physical features of OBSH were calculated using the quantum chemical calculations of Density Functional Theory (DFT). The analysis was carried out on the possible reaction path of OBSH molecule with OH radicals. Gauss View 5 and the Gaussian 09 programs were used for the calculation of optimized geometry and the geometric optimization for the determination of the lowest energy status. For the gas phase, activation energy for the estimated reaction paths was calculated and their most stable state from the thermodynamic perspective was determined. The aim of this study is to estimate the degradation mechanism of OBSH molecule in gas phase.

Keywords: OBSH, DFT, Gaussian 09, hydroxyl radical.

Introduction

Oxydibenzenesulfonyl hydrazide (OBSH), which is known with its chemical formula as $C_{12}H_{14}N_4O_5S_2$, is a colourless, crystalline solid foaming agent used for rubber and plastic and also as a polymer additive, and is known to be denser than water. Direct contact with OBSH may cause to irritation on skin, in eyes, or mucous membranes. Due to its being a toxic gas, OBSH affects people negatively when this chemical is inhaled. OBSH, which is used as the foaming agent, decomposes exothermically and releases nonpolar oligomers, N, and H_2O, in its foaming process[1,2].

Hydrazine derivatives, which also are available in some plants, have a widespread use in industry, agriculture and medicine. In scientific literature, there are many studies, which reveal that some hydrazine derivatives were found out to be potentially carcinogenic in animals, especially in mice. Nevertheless, studies on the potential carcinogenicity in mammalian cells have not been completed yet[3].

OBSH is an organic compound. As stated in many studies, organic contaminants are known to exist in water at very low concentrations. Thus, it is crucial that drinking water be purified from the organic contaminants. Solar light on earth helps water systems like lakes, rivers, etc. to be purified naturally. Large organic molecules are degraded into smaller basic molecules through sunbeams, and finally form CO_2, H_2O, other small molecules[4–6]. Organic compounds react with OH radical by undergoing photolysis, and this reaction is the most dominant reaction among dissipation reactions in the atmosphere. Biomolecules, which are hydroxyl scavengers at various speeds, are specific detectors for hydroxyl radical due to their ability of hydroxylation. Moreover, the repulsion of existent substituents, and the electron withdrawal lead to the position of the attack to the ring. The attack of any hydroxyl radical to an aromatic compound leads to a hydroxylated product to be formed, and these newly formed products may be much more harmful that their original product in the beginning of the process, thus it is essential that these

products be monitored[6,7–9].

In this study, the kinetics of the degradation reaction path of O molecule with OH radical was analysed theoretically through the density functional theory (DFT) method. Theoretical calculations were carried out at DFT/B3LYP/631G(d) level in gas-phase[10].

Computational models:

Mean bond distances and geometric parameters of the closed ring were used to form molecule models. Tetrahedral angles were used for the sp^3-hybridized carbon and oxygen atoms and 120° for the sp^2-hybridized carbon atoms was used in the computational modelling. The aromatic ring was left planar, excluding the position of attack. Since there was an alteration in the hybridization state of the carbon at the addition centre from sp^2 to sp^3, the attacking OH radical was estimated to form a tetrahedral angle with the C-H bond[6,11].

Molecular orbital calculations:

In photocatalytic degradation reactions of O molecule, it is possible that products more harmful than those in the original material could be formed. For this reason, it is crucial to apprehend the nature of the primary intermediate products before conducting a photocatalytic degradation reaction experimentally. Calculations carried out by quantum mechanical methods provide the most reliable and precise information. Hence, due to the yield produced being the same, photocatalytic degradation reactions of O molecule and its hydroxy derivatives were based on the direct reaction of these molecules with OH radical. With this aim, the kinetics of the reactions of O molecule with OH radical was theoretically analysed. The study was initiated with O molecule and then exposed to reaction with OH radical and the reaction yields were modelled in gas-phase. Experimental results in the scientific literature revealed that OH radical detaches a hydrogen atom from saturated hydrocarbons, and OH radical is added to unsaturated hydrocarbons and materials with this structure[6,12,13]. Therefore, possible reaction paths for the analysed reactions were calculated. In this study, primarily the conformation analyses of the foaming agent OBSH were conducted, and the conformers with the lowest energy, or in other words, the most stable ones were determined. Geometric optimizations of the molecule were carried out at DFT/

B3LYP/6-31G(d) level. As a result of the quantum chemical calculations, the geometric parameters, energy, enthalpy, and Gibbs-free energy, and also load density, and mulliken loads in gas-phase were determined[6,10].

Methodology:

The investigated reaction system was composed of OH radical, which are open-shell species. It is known that open-shell molecules cause severe problems in quantum mechanical calculations. The self-consistent field method (SCF) calculation will proceed for an open-shell case in the same way as for a closed-shell case. Nevertheless, because of two sets of equations having to be dealt with, at each iteration, the program has to consider, either simultaneously or successively, the closed-shell and the open-shell equations. In this respect, the computational burden could be two-times larger for an open shell than that for a closed-shell. Another point raised in connection with the optimization of the SCF process for open-shell molecules is the relative intricacy of the sequence of calculations for the closed-shell Hamiltonian and the open-shell Hamiltonian[14].

DFT methods, taking the electron correlation into account, use the precise electron density to calculate molecular properties and energies. Spin contamination does not affect them and hence, for calculations involving open-shell systems, they become favourable. DFT calculations were made by the hybrid B3LYP functional combining the HF and Becke exchange terms with the Lee-Yang-Parr correlation functional. In such calculations, it is the 6-31G(d) basis set that is used[6,10].

Results and discussion

According to Fig. 1 of O molecule, O_3, O_{32}, N_{33} and N_{35} molecules on the right, O_{23}, O_{24}, N_{25} and N_{27} molecules on the left, and O_{11}. When bond angles and bond lengths were investigated, values written bold in Table 1 gave preliminary information about the fragmentation sites of the molecule.

Bond lengths and bond angles of O molecule, which is analysed in this study, and its three stable fragments namely, O_1, O_2 and O_3 are given in this table. The bond lengths and angles with the highest value are bold written in this table. The probable stable fragmentation pathway of O molecule is given in Fig. 2.
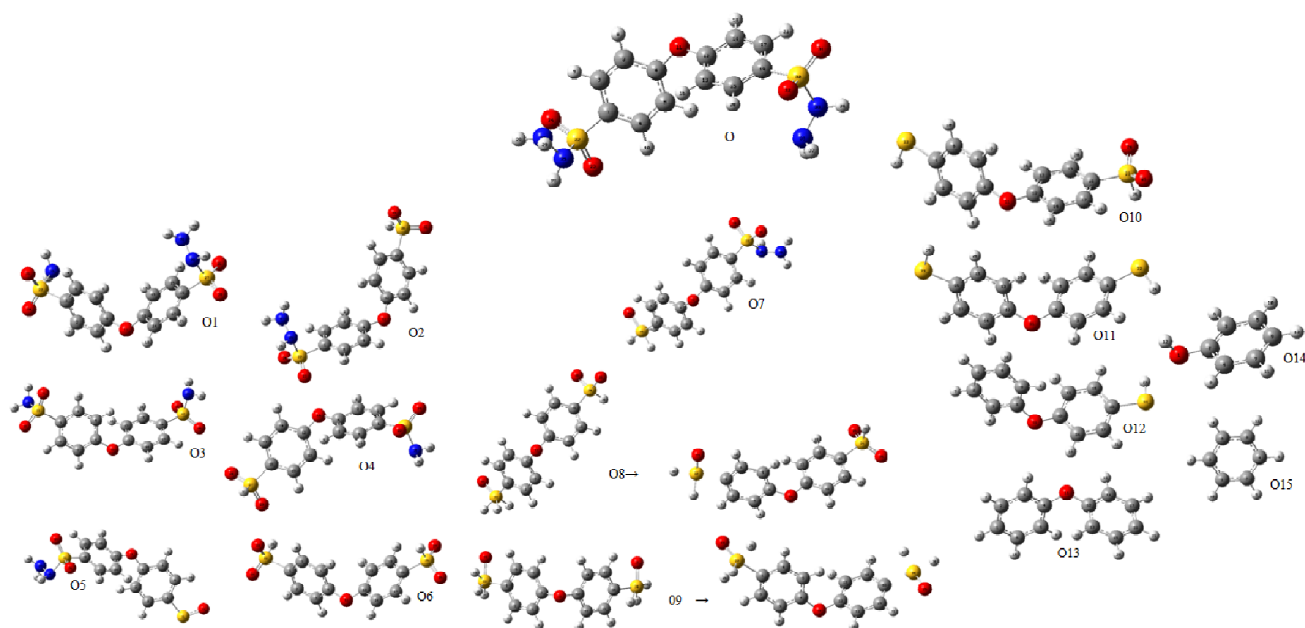
Fig. 1. Optimized figures of O molecule (yellow, sulphur; blue, nitrogen; white, hydrogen; red, oxygen; grey, carbon).

Table 1. Bond lengths and angles of some stable fragments of O molecule

O	Bond length (Å)	O	Bond angle (°)	O1	Bond length (Å)	O1	Bond angle (°)
$N_{33}N_{35}$	1.41245	$N_{35}N_{33}S_{30}$	**112.06538**	$N_{25}S_{22}$	**1.70068**	$N_{32}N_{30}S_{27}$	**112.06146**
$S_{30}N_{33}$	**1.71834**	$N_{33}S_{30}O_{31}$	103.40508	$N_{32}N_{30}$	1.41248	$C_{19}S_{27}O_{28}$	109.69545
$S_{30}O_{31}$	1.46640	$N_{33}S_{30}O_{32}$	110.36653	$N_{30}S_{27}$	**1.71806**	$C_{19}S_{27}O_{29}$	108.13353
$S_{30}O_{32}$	1.46700	$O_{32}S_{30}C_{19}$	108.14411	$S_{22}C_1$	1.78899	$N_{30}S_{27}O_{29}$	**110.38744**
$S_{30}C_{19}$	1.78407	$O_{31}S_{30}C_{19}$	109.70571	$S_{22}O_{24}$	1.46620	$N_{30}S_{27}O_{28}$	103.40950
$C_{12}O_{11}$	1.37797	$O_{31}S_{30}C_{19}$	109.70571	$S_{22}O_{23}$	1.46624	$C_1S_{22}O_{24}$	107.54988
C_4O_{11}	1.37748	$C_4O_{11}C_{12}$	**121.68182**	$S_{27}O_{28}$	1.46637	$C_1S_{22}O_{23}$	107.68583
$N_{25}N_{27}$	1.41250	$N_{27}N_{25}S_{22}$	**111.99521**	$S_{27}O_{29}$	1.46694	$C_4O_{11}C_{12}$	**121.70423**
$N_{25}S_{22}$	**1.71876**	$N_{25}S_{22}O_{23}$	103.39603	$S_{27}N_{19}$	1.78432	$O_{28}S_{27}O_{29}$	**121.15952**
$S_{22}C_1$	1.78372	$O_{31}S_{30}C_{19}$	109.70571			$O_{23}S_{22}O_{24}$	**122.52825**
O2	Bond length (Å)	O2	Bond angle (°)	O3	Bond length (Å)	O3	Bond angle (°)
$S_{30}C_{19}$	1.78564	$N_{27}N_{25}S_{22}$	**112.07913**	$S_{27}\text{-}N_{30}$	1.71000	$O_{28}S_{27}N_{30}$	109.47122
$S_{22}N_{25}$	**1.71730**	$O_{31}S_{30}O_{32}$	**122.69507**	$S_{27}\text{-}C_{19}$	1.78000	$O_{29}S_{27}N_{30}$	109.47122
$N_{25}N_{27}$	1.41252	$O_{23}S_{22}O_{24}$	**121.21582**	$O_{11}\text{-}C_{12}$	1.43000	$N_{25}S_{22}C_1$	109.47120
C_1S_{22}	1.78613	$C_4O_{11}C_{12}$	**121.63381**	$S_{22}\text{-}C_1$	1.78000	$C_1S_{22}O_{23}$	109.47123

When mulliken loads of O molecule given in Table 2 were analysed. Mulliken loads of the studied O molecule and all its fragments are given this table. The atoms with the highest electronegativity are bold written in the table. For example,

N_{27} and N_{35} are atoms with the highest electronegativity among all atoms with high electronegativity, and are marked as red in this Table 2.

Energy values in gas phase of the O molecule and its all
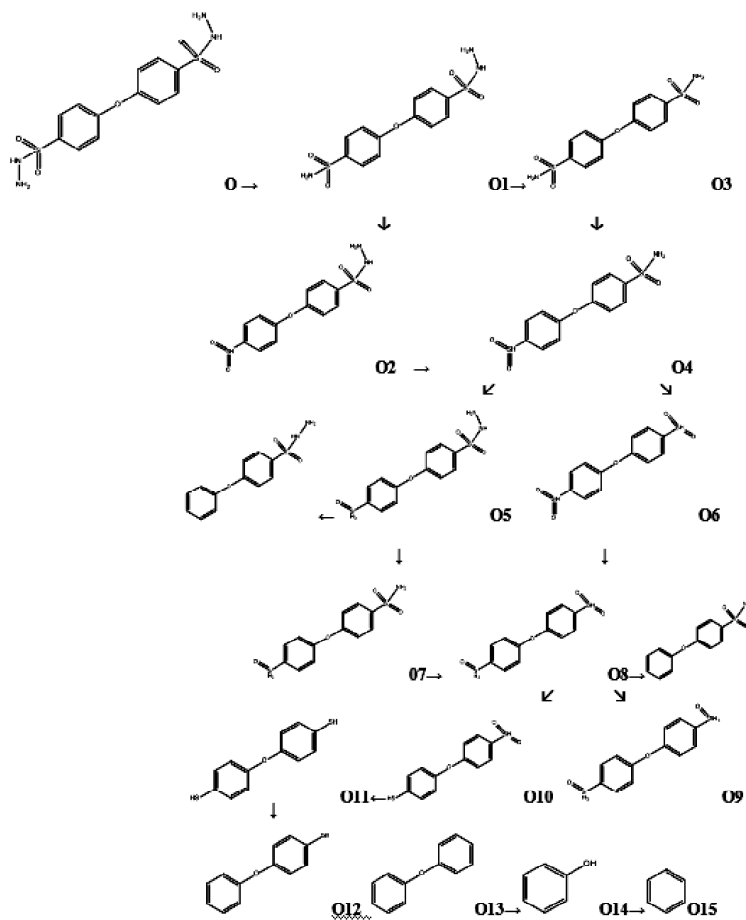
Fig. 2. Probable fragmentation paths of O molecule.

Table 2. Mulliken loads of studied fragments

O		O1		O2		O3		O4	
O_{11}	−0.564521	O_{11}	−0.564373	O_{11}	−0.562860	O_{11}	−0.564411	O_{11}	−0.562827
O_{23}	−0.545626	O_{23}	−0.536879	O_{23}	−0.543170	O_{23}	−0.531019	O_{23}	−0.536132
O_{24}	−0.532863	O_{24}	−0.533034	O_{24}	−0.531937	O_{24}	−0.537824	O_{24}	−0.529870
N_{25}	−0.564232	N_{25}	−0.815162	N_{25}	−0.565390	N_{25}	−0.815634	N_{25}	−0.815872
N_{27}	−0.590464	S_{27}	1.230531	N_{27}	−0.590923	S_{27}	1.169158	S_{27}	0.946383
O_{31}	−0.544736	O_{28}	−0.544662	S_{30}	0.946117	O_{28}	−0.531729	O_{28}	−0.511515
O_{32}	−0.533611	O_{29}	−0.533215	O_{31}	−0.513078	O_{29}	−0.537027	O_{29}	−0.512390
N_{33}	−0.564726	N_{30}	−0.564920	O_{32}	−0.511715	N_{30}	−0.815662		
N_{35}	−0.590546	N_{32}	−0.590550						
O5		O6		O7		O8		O9	
O_{11}	−0.569297	O_{11}	−0.560980	O_{11}	−0.568111	O_{11}	−0.567470	O_{11}	−0.568483
O_{22}	−0.545007	O_{23}	−0.510881	O_{22}	−0.543656	O_{23}	−0.543686	O_{23}	−0.549720
O_{24}	−0.547326	O_{24}	−0.509895	O_{24}	−0.530918	S_{24}	0.943833	S_{24}	0.509497
O_{25}	−0.536001	S_{25}	0.948051	O_{25}	−0.541531	O_{25}	−0.514614	O_{25}	−0.543899
N_{26}	−0.564121	O_{26}	−0.509899	N_{26}	−0.815581	O_{26}	−0.514906		
N_{28}	−0.589968	O_{27}	−0.510884	S_{28}	0.509536				

Table-2 (contd.)

O10		O11	O12	O13	O14
O_{11} −0.568989		O_{11} −0.576329	O_{11} −0.575676	O_{11} −0.575569	O_1 −0.664287
S_{22} −0.013311		S_{22} −0.030737	S_{22} −0.030487		
O_{24} −0.515220					
O_{25} −0.514728					

Table 3. Gibbs-free energy, enthalpy, and energy values (au) for the gas- phase of the degraded fragments of the O molecule

Gas	O	O1	O2	O3
ΔE (au)	−1856.687437	−1801.392479	−1746.043727	−1746.097532
ΔH (au)	−1856.686493	−1801.391535	−1746.042783	−1746.096588
ΔG (au)	−1856.763831	−1801.467134	−1746.114375	−1746.170572
	O4	O5	O6	O7
ΔE (au)	−1690.748730	−1671.897266	−1635.399688	−1616.602235
ΔH (au)	−1690.747786	−1671.896322	−1635.398744	−1616.601291
ΔG (au)	−1690.817239	−1671.967109	−1635.464691	−1616.670739
	O8	O9	O10	O11
ΔE (au)	−1561.254076	−1487.111509	−1485.043581	−1334.684513
ΔH (au)	−1561.253132	−1487.110565	−1485.042637	−1334.683569
ΔG (au)	−1561.318145	−1487.174532	−1485.104846	−1334.742610
	O12	O13	O14	O15
ΔE (au)	−936.500865	−538.317189	−307.349412	−232.143520
ΔH (au)	−936.499921	−538.316245	−307.348467	−232.142576
ΔG (au)	−936.553344	−538.364528	−307.383363	−232.175367

stable fragments are given in this table. As seen in this table, all fragments have negative values. Reaction pathways from O_1 to O_{15} are estimated through these energy values given in the Table 3.

Conclusions

The molecule was analysed whether stable fractions found through the analysis of bond lengths and angles shown in Table 1 were compatible with electrochemical values found in Table 3. In addition to predicting that the fragmentation occurring from the bond lengths starting from long to short ones, molecules are divided into fractions by electronegative atoms in molecules, bond lengths, bond angles and by taking into consideration the stable-close ring.

When bond angles and bond lengths were investigated, values written bold in Table 1 gave preliminary information about the fragmentation sites of the molecule. Due to the bond angles and bond lengths of bold written values being higher than the others, S_{22}, S_{30} and O_{11} were estimated to

be fragmented around S-N, S-C and C-O bonds. According to Fig. 1 of O molecule, O_3, O_{32}, N_{33} and N_{35} molecules on the right, O_{23}, O_{24}, N_{25} and N_{27} molecules on the left, and O_{11} in the centre have negative values when their mulliken loads given in Table 2 are analysed. O and N are electronegative atoms. When mulliken loads of O molecule given in Table 2 were analysed, it was determined that N_{27} and N_{35} were atoms with the highest electronegativity. Electronegativity ranking continued as N_{33}, O_{11}, N_{25}, O_{23}, O_{31}, O_{32}, O_{24} atoms respectively. Various fractions were obtained by fragmentation from bonds close to these atoms. N_{27} and N_{35} in Table 2 are the atoms with the lowest mulliken load on their O molecule. Therefore, the fragmentation process was started from these atoms. First, several variations of fragmentation from the N atoms at the terminal points were experimented.

For each fraction, electrochemical calculations within gaseous phase were analysed. ΔE energy, ΔH enthalpy and ΔG Gibbs free energy values given in Table 3 are stated for

each fragment separately. When ΔG Gibbs free values were analysed, it was seen that ΔG value of each fragmentation was negative. These results show that fragmentation occurred spontaneously. Fragments with the lowest electrochemical energy, in other words, the most stable fragments are O_1 with -1801.392479 au, O_3 with -1746.097532 au, and O_2 with 1746.043727 au, and O_4 with -1690.748730 au respectively.

The probable stable fragmentation pathway of O molecule is given in Fig. 2. In these probable pathways, fragmentation process was carried out from different electronegative parts of the molecule, and thermochemical values in each fragmentation were calculated. In these possible fragmentation pathways, OBSH molecule was fragmented into its smallest fragment; thus the fate of OBSH in nature was determined for further experimental studies.

Acknowledgements

References

1. B. A. Hunter and D. L. Schoene, *Ind. Eng. Chem.,* 1952, **44**, 119.

2. Y. F. Zhang, X. J. Wang, Z. G. Pan, C. M. Hong and G. F. Ji, *Journal of Applied Polymer Science*, 2015, **132**, 47.

3. H. Mori, S. Sugie, N. Yoshime, H. Iwata, A. Nishikawa, K. Matsukubo, H. Shimizu and I. Hirono, *Jpn. J. Cancer Res. (Gann)*, 1988, **79**, 204.

4. K. Verschueren, "Handbook of Environmental Data on Organic Chemicals", 2nd ed., Wiley, New York, 1996.

5. R. W. Matthews, D. Ollis and H. Al-Ekabi, "Photocatalytic Purification and Treatment of Water and Air", Elsevier Science, Amsterdam/New York, 1993, 121.

6. B. Eren, Y. Yalcin Gurkan, *JSCS*, 2017, **82**, 277.

7. V. G. Buxton, L. C. Greenstock, P. W. Helman and B. A. Hunter, *Journal of Physical and Chemical Reference Data*, 1988, **17**, 513.

8. M. Anbar and P. Neta, *Int. J. Appl. Radiat. Isot.*, 1967, **18**, 493.

9. B. Halliwell, M. Grootveld and J. M. C. Gutteridge, *Methods Biochem. Anal.*, 1998, **33**, 59.

10. Gaussian 09, Revision B.04, Gaussian, Inc., Pittsburgh, PA, 2009.

11. A. Hatipoglu, D. Vione, Y. Yalcin, C. Minero and Z. Cinar, *J. Photochem. and Photobiol.*, 2010, **215**, 59.

12. P. W. Atkins, "Physical Chemistry", 6th ed., Oxford University Press, New York, 1998.

13. K. Mierzejewska, J. Trylska and J. Sadlej, *J. Mol. Model.*, 2012, **18**, 2727.

14. H. F. Diercksen Geerd, B. T. Sutcliffe and A. Veillard, Computational Techniques in Quantum Chemistry and Molecular Physics, Proceedings of the NATO Advanced Study Institute held, Ramsau, Germany, 1974, 4-21.